Homology modeling of thermostable YdaP enzyme from Bacillus licheniformis

Article · January 2021

CITATION
1

READS
159

6 authors, including:

Joseph Lako
University of Juba, Juba City, South Sudan.
20 PUBLICATIONS **36** CITATIONS
SEE PROFILE

Jada Pasquale YENGKOPIONG
17 PUBLICATIONS **41** CITATIONS
SEE PROFILE

Clara Lumori
Wageningen University & Research
3 PUBLICATIONS **13** CITATIONS
SEE PROFILE

Justin Bruno Tongun
University of Bergen
20 PUBLICATIONS **249** CITATIONS
SEE PROFILE

Research Article

Homology modeling of thermostable YdaP enzyme from *Bacillus licheniformis*

Joseph Daniel Wani Lako[1], Kenneth L. L. Sube[2], Jada P. Yengkopiong[3], Clara S. G. Lumori[1], Justin B. Tongun[2], Don A. Cowan[4]

[1]Department of Biotechnology, School of Applied and Industrial Sciences, University of Juba, Juba, South Sudan, [2]Department of Biochemistry, School of Medicine, University of Juba, Juba, South Sudan, [3]Department of Biotechnology, College of Science and Technology, Dr. John Garang Memorial University of Science and Technology, Jonglei State, Bor Town, South Sudan, [4]Center for Microbial Ecology and Genomics, University of Pretoria, Pretoria, South Africa

ABSTRACT

Bacillus licheniformis YdaP gene encodes for pyruvate oxidase (EC: 1.2.3.3), a key enzyme which catalyzes the oxidative decarboxylation of pyruvate into acetate and CO_2. The objective of this study is to predict the YdaP protein structure, by comparison with known X-ray structures and using bioinformatics tools. The three-dimensional model structure of the *B. licheniformis* YdaP enzyme was constructed using the sequence of *L. plantarum* POX as the template. The model structure of *B. licheniformis* YdaP showed positional conservation of amino acid residues Asp313 and Ala314, compared with other members of the pyruvate oxidase family. The model structure of *B. licheniformis* YdaP showed that residues Met466, Ile467 and Glu470 were located on an α-helix connecting to loops in the active cavity. These residues are presumably critical for the catalytic activity of pyruvate oxidases, and have been proposed to be involved in substrate binding. The overall topology of the *B. licheniformis* YdaP was similar to known pyruvate oxidase crystal structures. The structure of the ThDP motif was identical to that found in the other pyruvate oxidases. However, analysis of the substrate binding cavity showed one major difference. Bulky hydrophobic amino acid residues Tyr469, His476 and Tyr479 formed part of active site cavity. In *L. plantarum* POX, these correspond to amino acid residues Trp479, Ile480 and Glu483. This observation suggested that these residues would negatively influence the accessibility of large substrates (e.g., aromatic) into the catalytic center. This information may assist in studies aimed at engineering the catalytic active site of the enzyme to improve accessibility of larger substrates to the active site.

Keywords: Active site, *Bacillus licheniformis*, Homology modeling, Protein structure, Pyruvate oxidase, Three-dimensional structure, YdaP enzyme

INTRODUCTION

The *Bacillus licheniformis* YdaP gene encodes for pyruvate oxidase (POX) (EC: 1.2.3.3) which is a peripheral membrane associated flavoprotein dehydrogenase that belongs to the thiamine diphosphate-dependent enzymes (Cronan, 1995). The thiamine diphosphate-dependent enzymes catalyze the oxidative decarboxylation of pyruvate to acetate and CO_2 (Lako *et al*., 2018). These enzymes are present in a variety of microorganisms from diverse ecosystems including *Escherichia coli* (Mather *et al*., 1982), *Corynebacterium glutamicum* (Schreiner and Eikmanns, 2005), *Staphylococcus aureus* (Patton *et al*., 2001; Zhang *et al*., 2017), *Aerococcus viridans* (Juan *et al*., 2007), and *Lactobacillus plantarum* (Sedewitz *et al*., 1984; Goffin *et al*., 2006; Lorquet *et al*., 2004). These enzymes have been widely studied due to their importance in biotechnological applications (Tomar *et al*., 2003) and have been well characterized (Lako *et al*., 2018). The interest in the POX (Pox; 1.2.3.3) is fueled by its potential capacity to produce important commodity chemicals including acetate in the presence of oxygen and inorganic phosphate. This enzyme requires thiamine diphosphate (ThDP), Flavin adenine diphosphate (FAD), and Mg^{2+} cofactors for its function in catalyzing the oxidative decarboxylation of pyruvate generating acetate (Tittmann *et al*., 2005). Characterization of the YdaP enzyme has revealed that it is typically composed of four identical subunits in their native state, with each subunit containing one molecule of the Mg^{2+} cofactor and ThDP. The subunit of this enzyme forms a lose dimer with ThDP and

Doi: 10.30954/2319-5169.01.2020.1

Submission: 23-05-2020 **Acceptence:** 27-06-2020
Received: 24-05-2020 **Published:** 30-06-2020

***Corresponding author:** Joseph Daniel Wani Lako, University of Juba, School of Applied and Industrial Sciences, Department of Biotechnology, Central Equatoria State, Juba Town, South Sudan; Phone: +211 924372730/+211 910083372; E-mail: jlako24@gmail.com

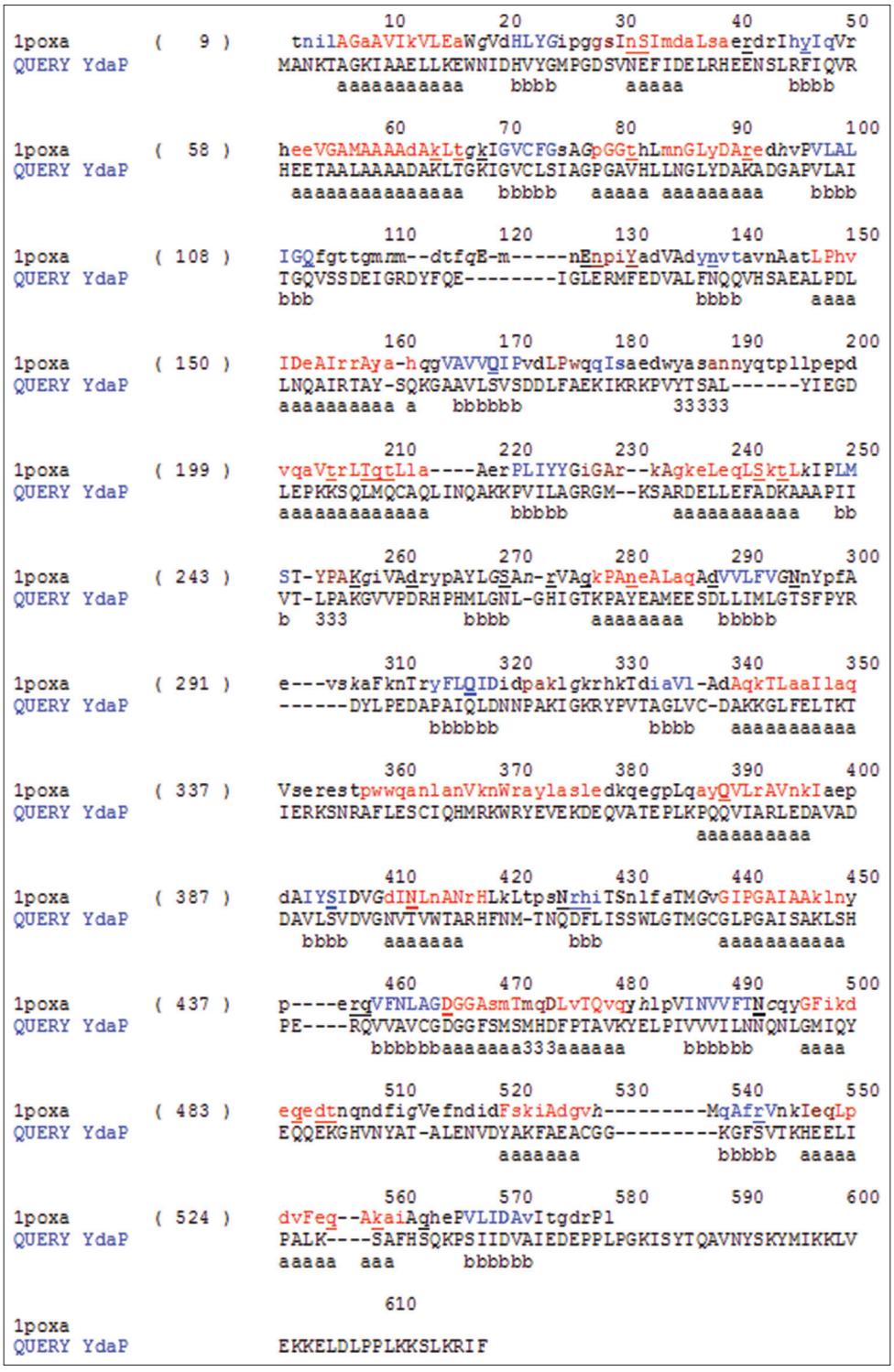

Figure 1: A secondary structure alignment of *Bacillus licheniformis* YdaP and *Lactobacillus plantarum* pyruvate oxidase (1 poxa). The alignment was used to generate the *B. licheniformis* YdaP 3D model

tight homotetramer in the presence of FAD. The enzyme has been expressed and purified and shown to have a molecular weight of 252 KDa (Lako *et al*., 2018), with seeming stability in purified form in the presence of ThDP. Several structured studies have been performed with the goal of defining the molecular basis of the functions of the family of these proteins (Johnson and Overigton, 1993; Muller *et al*., 1994; Juan *et al*., 2007). Most revealing were the two reports describing crystal structures of the POX (*L. plantarum*, PDB: accession number 2EZ9; *Aerococcus viridian*, and PDB: accession number IV5E). Comparative analysis of these structures reveals that the overall fold is conserved (Juan *et al*., 2007). The closest

structural homologue was identified as POX, PDB: 2EZ9 from *L. plantarum*, which shared 35% sequence identity to YdaP (Z-score >6.0) [Figure 1]. As a result PDB: 2EZ9 was selected as a template for the modeling of *B. licheniformis* YdaP protein. This enzyme represents one of the first moderately thermophilic *Bacillus* 9A that expresses a highly active, thermostable protein. YdaP enzyme exhibited a very wide range of substrate specificity. The gene encoding this enzyme has been cloned, expressed, purified, and characterized extensively (Lako *et al*., 2018). Furthermore, the structure shows extensive interactions in the subunit-subunit interface which is significantly different from the other group of POX and might be responsible for the variation in biochemical properties between the species (Muller *et al*., 1994). In this study, the three-dimensional structures of the POX: 2EZ9 and YdaP were generated using the homology modeling techniques (Sutcliffe *et al*., 1987; Martin *et al*., 1994; Muller *et al*., 1994; Sănchez and Săli, 1997) to compare the quaternary structures of these bacterial POXs with respect to the enzyme substrate interaction and subunit-subunits interface that might be related to the different biochemical characteristics (Bowie and Eisenberg, 1991).

MATERIALS AND METHODS

Modeling of the YdaP Enzyme *B. licheniformis* and POX of *L. plantarum*

The sequence alignment of the deduced amino acids of *B. licheniformis* YdaP and the *L. plantarum* POX (GenBank: *B. licheniformis*, accession number: CBE70488 and *L. plantarum*, accession number: P 37063, respectively) [Figure 1] were used for model building using the MODELLER 9v4 program (Blundell *et al*., 1987; Šali and Blundell, 1993; Šali and Overigton, 1994; ; Šali *et al*., 1995) The closest structural homologue was identified as PDB: 2EZ9 from *L. plantarum*, which shared 35% sequence identity to YdaP (Z-score > 6.0) (Figure 2A). As a result PDB: 2EZ9 was selected as a template for the modelling of *B. licheniformis* YdaP protein [Figure 2B]. A superimposition of the structural model of *B. licheniformis* YdaP with *L. plantarum* POX shows overall structural similarity [Figure 2c]. YdaP shares 35% sequence identity with *L. plantarum*. The assessment and validation of the model stereochemistry were carried out using the RAMPAGE (Lovell *et al*., 2001) software. This program analyses and plots Ψ and Ø angles in the structure. The Ψ, Ø plot for the model structure is considered as a reliable method of evaluating torsion angles and has become an important strategy for validation of protein model structures (Kleywegt and Jones, 1998). Overall Ψ, Ø distribution in *B. licheniformis* YdaP structure was shown to be good [Figure 3].

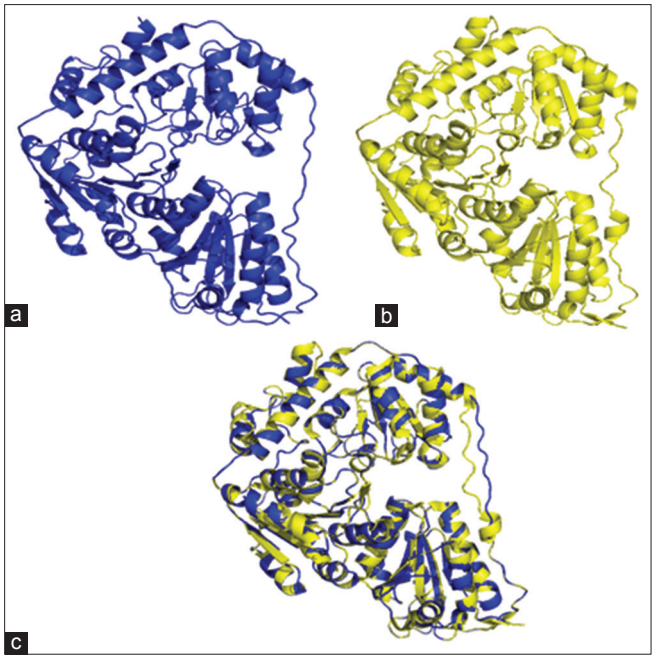

Figure 2: (a) Cartoon representation of the 3D crystal structure of the *Lactobacillus plantarum* pyruvate oxidase subunit; (b) homology structure model of *Bacillus licheniformis* YdaP subunit; (c) superimposed structural models of *L. plantarum* POX and *B. licheniformis* YdaP 3D

RESULTS AND DISCUSSION

Description of the Model Structure

The *B. licheniformis* YdaP model suggested that the protein monomer was comprised three distinct domains, separated by loops [Figure 4]. These domains were identified using homology search of the secondary structure alignment between *B. licheniformis* YdaP and *L. plantarum* POX. The entire globular structure consisted of 22 α-helices and 21 β-sheets. The N-terminal domain was commenced with a

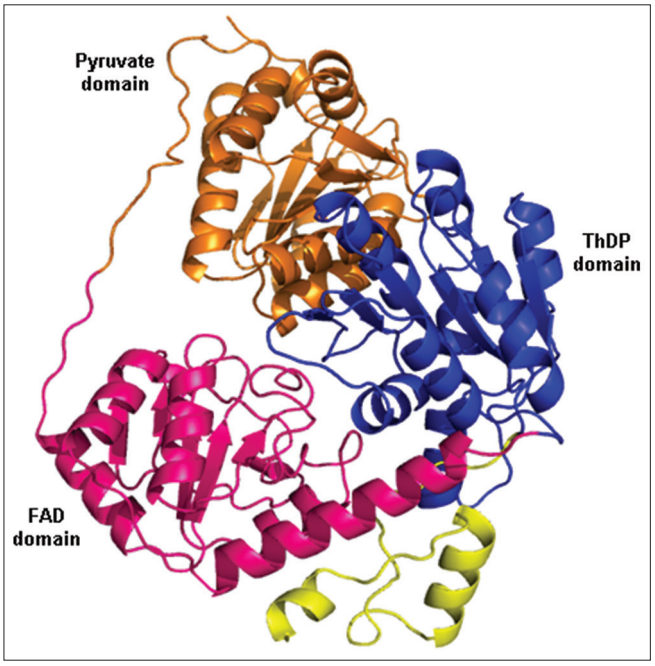

Figure 3: Cartoon representation of the YdaP subunit

long core domain stretching from residues 3–183 (in orange). This was followed by the FAD domain, which spans residues 184–351 (in pink). These domains lead to the long ThDP domain, stretching between residues 352 and 550 (in blue). The C-terminal primary structure consists between residues 550 and 572 (in yellow) was thought to be a membrane anchor (Neumann *et al*., 2008). These features are found in all elucidated POX structures (Muller and Schulz, 1993; Neumann *et al*., 2008; Wille *et al.,* 2006).

The cofactor FAD was predicted to bind to the YdaP enzyme at Asp313 and Ala314 in the FAD domain [Figure 5], which corresponded to residues Asp323 and Ala324 in *L. plantarum* POX and appeared to be conserved in both structures. This prediction was based on the fact that these residues were highly conserved in POXs from different organisms (Wille *et al*., 2006).

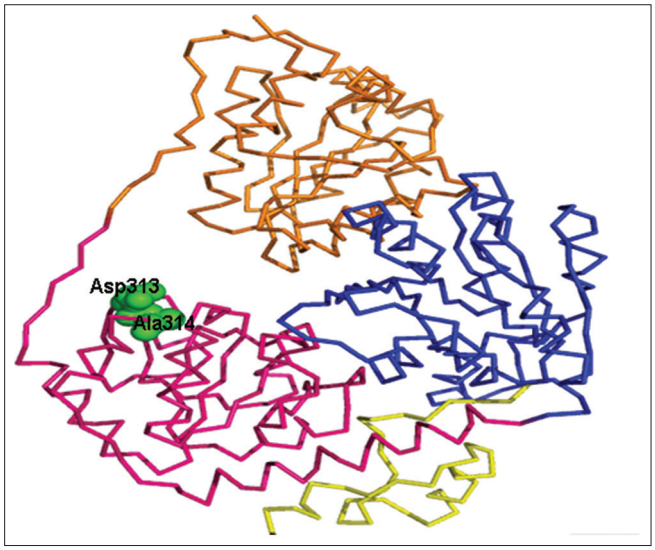

Figure 4: Ribbon representation of residues Asp313 and 314 (in green) predicted to be involved in binding to the flavin adenine diphosphate cofactor

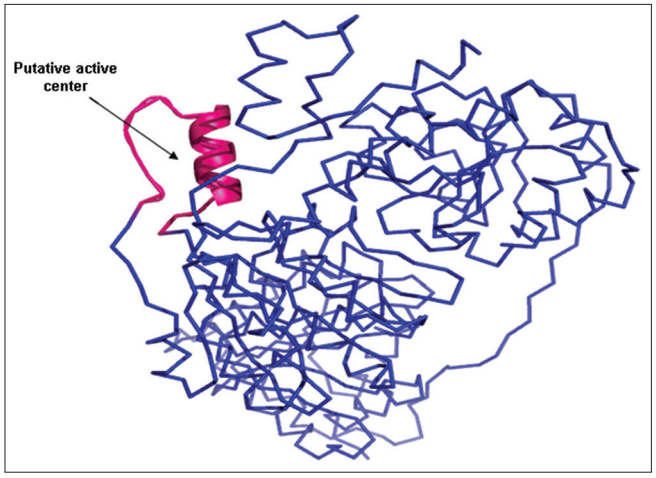

Figure 5: Proposed active center of *Bacillus licheniformis* YdaP

Topological Description of the YdaP Model

The model structure of YdaP displayed an overall topology similar to the experimentally determined structures of POX from *L. plantarum* (Bajorath *et al*., 1994; Wille *et al*., 2006), *E. coli,* and *A. viridans* (Juan *et al*., 2007). The active site structure showed considerable topological homology in both models and template structures (Sánchez and Šali, 1997; Shi *et al*., 2001). However, the YdaP substrate-binding pocket was similar to the equivalent site in *L. plantarum* POX, supporting experimental data showing that YdaP accepted pyruvate and some larger branched chain substrates (Lako *et al*., 2018). The ThDP motifs of both model structures exhibited a similar structure, their sequences homology of 52%. This observation suggests that the two enzymes are closely related and could indicate an evolutionary relationship (Arnold, 1998) [Figure 6].

Disulfide Bridges

A detailed analysis of the overall model structure of *B. licheniformis* YdaP performed using the SSprov 4.5

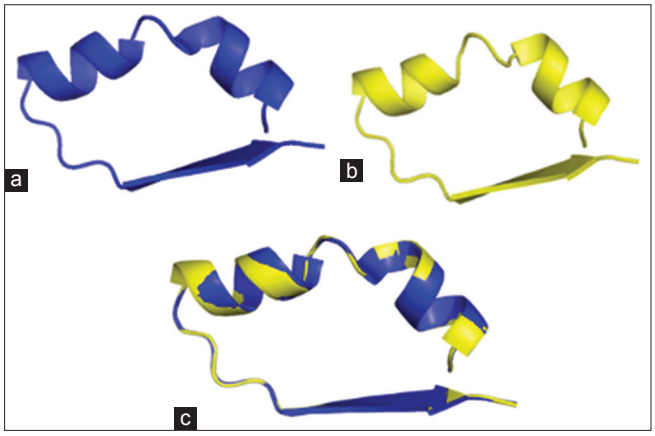

Figure 6: Cartoon representation of (a) ThDP motif of YdaP from *Bacillus licheniformis*; (b) ThDP motif of *Lp*POX from *Lactobacillus plantarum*; (c) superimposed ThDP motifs of both structure models

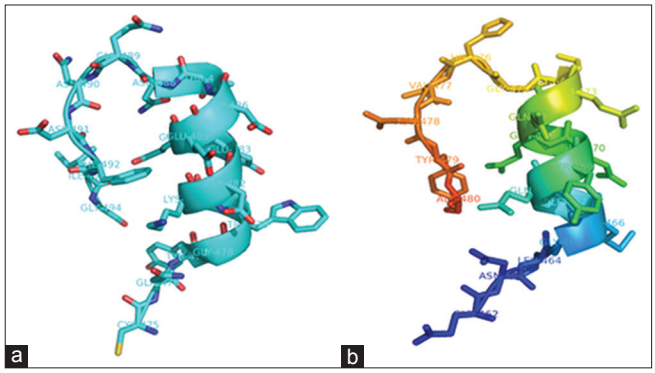

Figure 7: Representation of active center of (a) *Lactobacillus plantarum* pyruvate oxidase; (b) *Bacillus licheniformis* YdaP and residues thought to be involved in catalytic activity

SCRATCH protein predictor (/www.ics.uci.edu/~baldig/scratch/explanation.html) revealed the presence of seven cysteine residues (C72, C196, C312, C337, C411, C432, and C495). Cysteines C312 and C337 and C411 and C432 were predicted to form disulfide bonds. However, the YdaP structure model predicted the distances between these cysteine residues to be approximately 3.5 Å, compared to 2.0 Å for typical disulfide bonds, suggesting that they do not form the disulfide bonds *in vivo*. It is known that disulfide bonds serve the critical function of stabilizing protein fold. Furthermore, it also plays a key role in oxidative, heat, and toxic element stresses (Leichert *et al*., 2003).

Catalytic Site Residues

The *B. licheniformis* YdaP showed considerable homology to the *L. plantarum* POX in the catalytic center [Figure 7]. Putative active site residues were identified in the YdaP model structure [Table 1], the putative active center was made up of a α-helix and two loops (Johnson *et al*., 1994; Jones, 1999), which were located at the subunit interface (Rapp and Friesner, 1999). In the model structure of *B. licheniformis* YdaP, the extended curved accessible channel was identified [Figure 7] and this channel was suggested to allow the accessibility of the substrate into the active site. The amino acid residues of this channel region were relatively less conserved (20%) in the structures of both YdaP (target sequence) and POX from *L. plantarum* (template sequence) (Wille *et al*., 2006). The residues Ile538, Ser539, Tyr540, Thr541, Val544, and Asn545 were potentially involved in the YdaP substrate binding site [Figure 8]. However, in *L. plantarum* POX these residues were located in different positions compared to *B. licheniformis* YdaP. There were considerable differences in the conservation of the substrate binding residues including Lys554, Leu555, Arg556, Leu557, Ala560, and Met561 [Figure 8], which were found in *L. plantarum* POX (Wille *et al*., 2006).

The 3D structural model of YdaP of *B. licheniformis* was constructed based on the closest similarity to the experimentally determined structure of *Lp*POX (Johnson *et al*., 1994; Wille *et al*., 2006). The structural model generated was assessed and it revealed to be in a good agreement with template structure suggesting the accuracy spectrum of the *B. licheniformis* YdaP model.

Active site residues were shown to be conserved among the two proteins except for Met466 of *B. licheniformis* YdaP which correspond to Trp479 in *L. plantarum* POX [Table 1] as well as in other homologues; however, the substrate binding residues have low conservation. The residues are clearly localized at the interface of the *B. licheniformis* YdaP subunit. Inspection of the active site residues revealed that Met466, Ile467, and Gln471 were located in the active site cavity. The active site residues were found to be similar in *B. licheniformis* YdaP compared to the *L. plantarum* POX [Table 1] which may possibly allow accessibility of other substrates. The classical features of *B. licheniformis* YdaP, include ThDP motif signature, catalytic active site, and disulfide bonds, were predicted and evaluated.

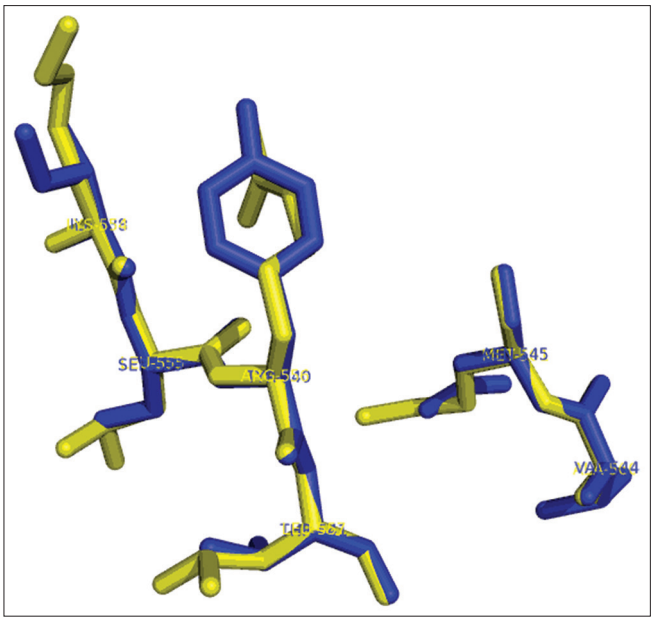

Figure 8: Stick representation of superimposition of residues involved in substrate binding site of *Bacillus licheniformis* YdaP (in blue) and *Lactobacillus plantarum* pyruvate oxidase (in yellow)

Table 1: Comparison of active site residues between *Lactobacillus plantarum* POX and *Bacillus licheniformis* YdaP

*Lp*POX	YdaP
Glu59	Glu52
His89	His82
Phe121	Phe114
Gln122	Gln115
Val376	Val364
Trp479	Met466
Ile480	Ile467
Glu484	Glu471

POX: Pyruvate oxidase

The YdaP model structure suggests that the catalytic cavity comprised Met466, Ile467, Gln468, Gly469, Lys470, Gln471, Gln472, and Glu473 which were located on the α-helix of the active site cavity, while residues Lys474, Gly475, His476, Val477, Asn478, Tyr479, and Ala480 were present on the loop on the opposite site of the catalytic cavity. Overall comparison of the both structures of *B. licheniformis* YdaP and *L. plantarum* POX, beside the arrangement of the active center residues showed that there was some level of variation on residues conservation. However, the active center exhibited consistency on structural basis compared to the *Lp*POX template structure [Figure 7]. Interestingly, the model structure prediction did not provide adequate details of catalytic mechanism of this group of enzymes. Therefore, crystal structure data are required to elucidate on the catalytic mechanisms of YdaP protein. The presence of seven cysteine residues within the YdaP protein

suggested that the *B. licheniformis* YdaP could form disulfide bonds. However, distance prediction of disulfide bonds by the *B. licheniformis* YdaP structure model was not appropriate for formation of the disulfide bonds (~2.0 Å). Despite the utilization of the detergent (1% Triton X-100) for the YdaP enzyme activation, there was no role played by it as reducing agent. Therefore, it can be concluded that Triton X-100 did not affect the formation of the disulfide bonds (Lako *et al*., 2018).

CONCLUSION

The comparative modeling strategy could provide useful information for improving the characteristics of the YdaP protein, particularly in the identification of the active site residues [Table 1]. The YdaP model structure showed that Met466 Ile467 and Glu471 located in the catalytic cavity are believed to be involved in catalytic activity. However, Glu52, His82, Phe114, and Gln115 appeared to be located on the surface, played an important role in catalytic activity of *B. licheniformis* YdaP. These predictions provided some basic information that could be useful for future studies of particular residues which might be a potential target for site-directed mutagenesis studies for the improvement of the activity of the enzyme (Arnold, 1998).

ACKNOWLEDGMENT

The authors gratefully would like to acknowledge TMO Renewable and the National Research Foundation (NRF), South Africa for the financial support of this project and without these support we would not have made this study successful.

Financial Support and Sponsorship

Nil.

Conflicts of Interest

The authors declare that there is no conflict of interest in this work.

REFERENCES

Arnold, F.H. 1998. Design by directed evolution. *Acc. Cashem. Res*., 31, 125-131.

Bajorath, J., Stenkamp, R. and Aruffo, A. 1994. Knowledge-based model building of proteins: Concepts and examples. *Protein Sci*., 2, 1798-1810.

Blundell, T.L., Sibanda, B.L., Sternberg, M.J.E. and Thornton, J.M. 1987. Knowledge-based prediction of protein structure and the design of novel molecules. *Nature*, 326, 347-352.

Bowie, J.U., Lüthy, R. and Eisenberg, D. 1991. A method to identify protein sequences that fold into a known three-dimensional structure. *Science*, 253, 164-170.

Chang, Y.Y. and Cronan, J.E., Jr. 1995. Detection by site-specific disulfide cross-linking of a conformational change in binding of *Escherschia* coli pyruvate oxidase to lipid bilayers. *J. Bio. Chem*. 270, 7896-7901.

Goffin, P., Muscariello, L., Lorquet, F., Stukkens, A., Prozzi, D., Sacco, M., Kleerebezem, M. and Hols, P. 2006. Involvement of pyruvate oxidase activity and acetate production in the survival of *Lactobacillus plantarum* during the stationary phase of aerobic growth. *Appl. Environ. Microbiol*., 72, 7933-7940.

Johnson, M.S. and Overigton, J.P. 1993. A structural basis for sequence comparisons: An evaluation of scoring methodologies. *J. Mol. Biol*., 233, 716-738.

Johnson, M.S., Srinivasan, N., Sowdhamini, R. and Blundell, T.L. 1994. Knowledge-based protein modelling. *Crit. Rev. Biochem. Mol. Biol*., 29, 1-68.

Jones, D.T. 1999. GenTHREADER: An efficient and reliable protein folds recognition method for genomic sequences. *J. Mol. Biol*., 287, 797-815.

Juan, E.C.M., Hoque, M.M., Hossain, M.T., Yamamoto, T., Imamura, S., Suzuki, K., Sekiguchi, T. and Takénaka, A. 2007. The structures of pyruvate oxidase from *Aerococcus viridans* with cofactors and with a reaction intermediate reveal the flexibility of the active-site tunnel for catalysis. *Acta Crystallogr. Sect. F Struct. Biol. Cryst. Commun*., 63, 900-907.

Kleywegt, G.J. and Jones, T.A. 1998. Phi/psi-chology: Ramachandran revisited. *Structure*, 4, 1395-1400.

Lako, J.D.W., Yengkopiong, J.P., Stafford, W.H.L., Tuffin, M. and Cowan, D.A. 2018. Cloning, expression and characterization of thermostable YdaP from *Bacillus licheniformis* 9A. *Acta Biochim. Pol*., 65, 59-66.

Leichert, L.I.O., Scharf, C. and Hecker, M. 2003. Global characterization of disulfide stress in *Bacillus subtilis*. *J. Bacteriol*., 185, 1967-1975.

Lorquet, F., Goffin, P., Muscariello, L., Baudry, J.B., Ladero, V., Sacco, M., Kleerebezem, M. and Hols, P. 2004. Characterization and functional analysis of the poxB gene, which encodes pyruvate oxidase in *Lactobacillus plantarum*. *J. Bacteriol*., 186, 3749-3759.

Lovell, S.C., Davis, J.W., Arendall, W.B. 3rd., de Bakker, P.I., Word, J.M., Richardson, M.G. and Richardson, J.S. 2001. Structure validation by Calpha geometry phi, psi and Cbeta deviation. *Proteins*, 50, 437-450.

Martin, A.C.R., MacArthur, M.W. and Thorton, J.M. 1997. Assessment of comparative modeling in CASP2. *Proteins*, 1, 14-28.

Mather, M., Schopfer, L.M., Massey, V. and Gennis, R.B. 1982. Studies of the flavin adenine dinucleotide binding region in *Escherichia coli* pyruvate oxidase. *J. Biol. Chem*., 257, 12887-12892.

Muller, Y.A. and Schulz, G.E. 1993. Structure of thiamine and flavin-dependent enzyme pyruvate oxidase. *Science*, 259, 965-967.

Muller, Y.A., Schumacher, G., Rudolph, R. and Schulz, G.E. 1994. The refined structures of a stabilized mutant and of wild-type pyruvate oxidase from *Lactobacillus plantarum*. *J. Mol. Biol*., 237, 315-335.

Neumann, P., Weidner, A., Pech, A., Stubbs, M.T. and Tittmann, K. 2008. Structural basis for membrane binding and catalytic activation of the peripheral membrane enzyme pyruvate oxidase from *Escherichia coli*. *Proc. Nat. Acad. Sci*., 105, 17390-17395.

Patton, T.G., Rice, K.C., Foster, M.K. and Bayles, K.W. 2005. The *Staphylococcus aureus cidC* gene encodes a pyruvate oxidase that affects acetate metabolism and cell death in stationary phase. *Mol. Microbiol,* 56, 1664-1674.

Rapp, C.S. and Friesner, R.A. 1999. Prediction of loop geometries using a generalized Born model of solvation effect. *Proteins*, 35, 173-183.

Šali, A. and Blundell, T.L. 1993. Comparative protein modeling by satisfaction of spatial restraints. *J. Mol. Biol*., 234, 779-815.

Šali, A. and Overington, J.P. 1994. Derivation of rules for comparative protein modeling from a database of protein structure alignments. *Protein Sci*., 3, 1582-1596.

Šali, A., Potterton, L., Yuan, F., Vlijmen, H. and Karplus, M. 1995. Evaluation of comparative protein structure modeling by MODELLER. *Proteins*, 23, 318-326.

Sánchez, R. and Šali, A. 1997. Advances in comparative protein-structure modeling. *Curr. Opin. Struct. Biol*., 7, 206-214.

Sănchez, R., Ya, B.A., Feyfant, E. and Šali, A. 1997. Homology protein structure modeling. *Trans. Am. Cryst. Assoc*., 32, 81-91.

Schreiner, M.E. and Eikmanns, B.J. 2005. Pyruvate: Quinone oxidoreductase from *Corynebacterium glutamicum*: Purification and biochemical characterization. *J. Bacteriol*., 187, 862-871.

Sedewitz, B., Schleifer, K.H. and Gotz, F. 1984. Purification and biochemical characterization of pyruvate oxidase from *Lactobacillus plantarum*. *J. Bacteriol*., 160, 273-278.

Shi, J., Blundell, T.L. and Mizuguchi, K. 2001. Sequence structure homology recognition using environment-specific substitution tables and structure-dependent gap penalties. *J. Mol. Biol*., 310, 243-257.

Sutcliffe, M.J., Hanseef, I., Carney, D. and Blundell, T.L. 1987. Knowledge based modelling of homologue proteins. Part I. Three dimensional frameworks derived from the simultaneous superposition of multiple structures. *Protein Eng*., 1, 377-384.

Tittmann, K., Wille, G., Golbik, R., Weidner, A., Ghisla, S. and Hübner, G. 2005. Radical phosphate transfer mechanism for the thiamin diphosphate and FAD-dependent pyruvate oxidase from *Lactobacillus plantarum*. Kinetics coupling of intercofactor electron transfer with phosphate transfer to acetyl-thiamin diphosphate via a transient FAD semiquinone/hydroxyethyl-ThDP radical pair. *Biochemistry*, 44, 13291-13303.

Tomar, A., Eiteman, M.A. and Atman, E. 2003. The effect of acetate pathway mutations on the production of pyruvate in *Escherichia coli*. *Appl. Microbiol. Biotechnol*., 62, 76-82.

Wille, G., Meyer, D., Steinmetz, A., Hinze, E., Golbik, R. and Tittmann, K. 2006. The catalytic cycle of a thiamin diphosphate enzyme examined by cryocrystallography. *Nat. Chem. Biol*., 2, 324-328.

Zhang, X., Kenneth, W. and Bayles, S.L. 2017. *Staphylococcus aureus* CidC is a pyruvate: Menaquinone oxidoreductase. *Biochemistry*, 56, 4819-4829.

How to cite this article: Lako, J.D.W., Sube, K.L.L., Yengkopiong, J.P., Lumori, C.S.G., Tongun, J.B. and Cowan, D.A. 2020. Homology modeling of thermostable YdaP enzyme from *Bacillus licheniformis*. *Int. J. Bioinform. Biol. Sci*. 8(1), 6-12.